THE THREE DIMENSIONAL SIMULATING STUDY OF THE FLOW AND HEAT TRANSFER IN DETACHED VEHICULAR COOLING-COMPARTMENT

Yuqi H.* , Xiaoli Y., Rui H., and Zhentao L.
*Author for correspondence
Power Machinery and Vehicular Engineering Institute,
Zhejiang University,
Hangzhou 310027,
P.R.China
Abbreviation E-mail: huangyuqi@zju.edu.cn

ABSTRACT

To explore the internal flow distributions and heat transfer mechanism in detached cooling-compartment, two three-dimensional models both including the heat exchangers and a full-sized fan model were established and analyzed in this paper. According to the study, the opposite model, on which the heat exchangers were located separately and close to the inlets, was considered to be more efficient. Besides, the opposite arrangement in detached cooling-department offered the possibility to control the mass flow on each heat exchanger independently, which could further increase the cooling efficiency. It deserves more attentions in the future.

INTRODUCTION

In order to fulfill the increasing requirements on the automobile dynamic, economic, and the comfortableness, lots of components, such as intercooler, air-conditioning condenser, radiator, oil cooler, electronic fan, variable speed pump, and smart thermostat etc. are assembled in the vehicular cooling system. For this reason, the cooling system turns into more and more complex.

The traditional cooling system is arranged in tandem, where the air as the cooling medium flows past several heat-exchangers one by one with the action of fan and vehicular movement. And it is located in the engine cabin, crowed with the engine, battery, transmission, and other accessories for saving space. There are two potential disadvantages in this kind of traditional cooling systems although it has the great advantages such as compact and convenient assembly. The first one is the disequilibrium of the cooling power among the heat exchangers. The cooling air passed the downstream heat exchanger has been largely heated, thus the cooling capability would be decreased accordingly. The second one is the non-adjustable of the frontal area and cooling performance. At some particular working conditions, one or two of the heat exchangers, such as air-conditioning condenser and intercooler, might be in downtime, there is no necessary to cooling these modules at the moment, but the cooling air still passes the way and creates same energy consumption.

NOMENCLATURE

f	[-]	Friction factor
k	[-]	Turbulence kinetic energy
ε	[-]	Turbulence dissipation rate
G_k	[-]	Generation of turbulence kinetic energy
C^*	[-]	Heat capacity ratio
NTU	[-]	The number of transfer units
$C_{\min}$	[J/(kg·K)]	The smaller heat capacity rate for the hot and cold fluids
$C_{\max}$	[J/(kg·K)]	The larger heat capacity rate for the hot and cold fluids
q_{micro}	[w]	The heat transfer rate of each sub-element
q_{total}	[w]	The total heat flux of the heat exchanger
E	[-]	Effectiveness
$\vec{v}_r$		The reference velocity vector in moving coordinate systems
$\vec{v}$		The velocity vector in absolute coordinate system
$\vec{v}_t$		The movement of moving coordinate system
$\vec{\omega}$		The angular speed of a rotation
ρ	[kg/m^3]	Density
μ	[Pa·s]	Dynamical viscosity

Considering these disadvantages, there is a tendency to separate the cooling system from the engine and other accessories, build a detached cooling compartment in some kind of bus and armored vehicle. On this condition, the cooling package can be arranged not only in the front of vehicle, but also in the rear of the vehicular body. Lisa *et al* [1] have investigated the effects of the cooling package positions. In their models, the rearward installation of the cooling package could decrease the drag at low velocities, but higher fan speed was required to reach the same cooling performance as frontward installation. By changing the cooling module position, the vehicle design and the area at the engine compartment would be more flexible. Mahmoud *et al* [2] have discussed the blockage effects imposed by engine in the cooling package. Their test results showed that by minimizing the blockage (increasing the distance between cooling package and engine), the air flow rate through the heat exchanger was increased, and the cooling performance was obvious improved. Based on these studies, the developments of detached cooling compartment by separating the cooling modules from the engine cabin have the realistic significance.

Figure 1 shows a common detached cooling compartment in the rear of bus, where the wind inflow through the side grills, and exhausts by rear fans. This kind of cooling compartments cannot run without the working of aspirated fans, but it enables the heat exchangers and fan be constructed in a new way. Figure 2 displays the sketch of an idealistic detached cooling compartment[3,4]. The related patent has been issued in China. The heat exchangers were arranged separately within enough space, thus there was no downstream heat exchanger any more.

The cooling performance of one module wouldn't be influenced by the other one. The flow resistance also could be easily controlled by locating shutters behind the heat exchangers. Then the air flow rate and cooling performance of each heat exchanger was able to be adjusted individually at any time.

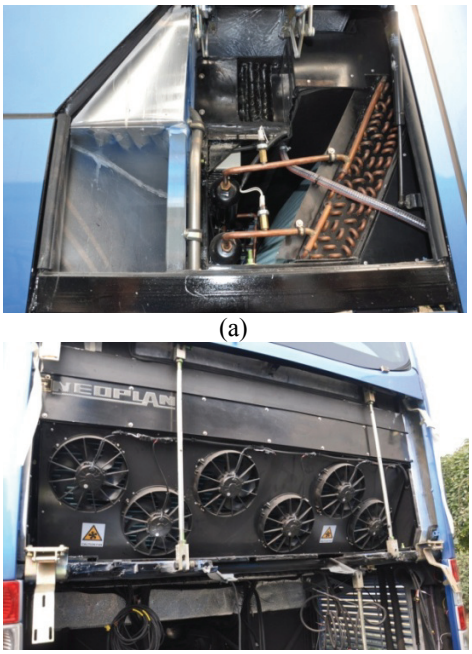

(a)

(b)

Figure 1 The photos of detached cooling compartment. (a) Side view, (b) Back view

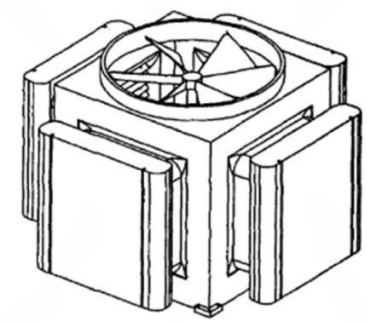

Figure 2 Sketch of an individual cooling compartment

Although the detached cooling compartment has been widely adopted in commercial vehicles, but the studies on its flow and heat transfer characteristics have not been carried extensively. In order to explore the internal flow distribution, two different three-dimensional models both including the heat exchangers and fan are established, numerical simulated, and analyzed here. The performances of heat dissipations were discussed to compare the influence by various arrangements. Commercial computational fluid dynamic (CFD) codes ANSYS FLUENT 14.5 based upon the finite volume method was used to make the simulation.

THE SIMULATING MODELS

Two various models as shown in Figure 3 are established to study the flow and heat transfer in the detached cooling-compartment. The fan adopted here is an aspirated fan. The inlets highlighted in blue are located in the left and right side of fan, and the outlet marked by grey is arranged exactly behind the fan. Except the inlets and outlet, the box is airtight. The initial velocity in both inlets are setting as zero, flows are only driven by the fan. Red blocks in the box represented the heat exchangers (HE), which are numbered by HE1 and HE2. The parameters adopted in HE1 are based on an intercooler with some tested results, and the parameters in HE2 are calculated by the tests of a typical radiator. The definitions of HE1 and HE2 in both models are the same respectively. In Model A, the heat exchangers are located separately and close to the inlets, we call it 'opposite model'. Yet in Model B, two heat exchangers are arranged adjacently and parallel to the fan. It is named 'parallel model' here.

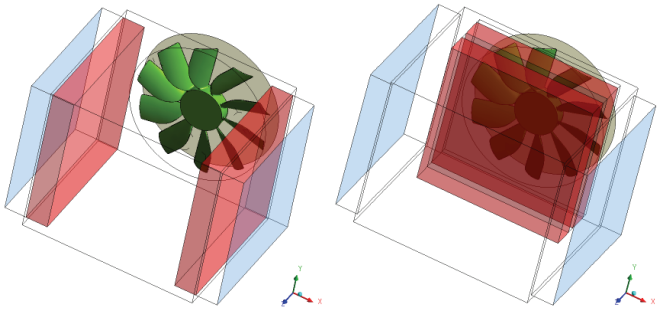

(a) (b)

Figure 3 The simulating models of detached cooling-compartment. (a) Model A, Opposite model, where the HE1 is in the right side and HE2 in left; (b) Model B, Parallel model, the HE1 is in the outside and the HE2 is closer to the fan.

Many assumptions based on the calculation requirements and model characteristics are proposed: the flow is steady, the cold mediums are incompressible ideal gas whose density only varied with temperature, and the physical properties of hot mediums are not changed in the simulation. Approximately 2.4 million mixture elements are generated for this model. It takes about 4h for calculation on a super-computer with 16 CPUs in each case.

Turbulence Model

The standard k - ε turbulence model with shear flow corrections is used to deal with high-speed turbulent flow problems. The second order upwind difference scheme (UD) is adopted for the momentum, energy and turbulence equations. The turbulence kinetic energy, k and its dissipation rate, ε, are obtained from the following transport equations:

$$\partial(\rho k)/\partial t + \partial(\rho k u_i)/\partial x_i = \partial[(\mu + \mu_t/\sigma_k)\partial k/\partial x_j]/\partial x_j + \rho G_k - \rho\varepsilon \quad (1)$$

$$\partial(\rho\varepsilon)/\partial t + \partial(\rho\varepsilon u_i)/\partial x_i = \partial[(\mu + \mu_t/\sigma_\varepsilon)\partial\varepsilon/\partial x_j]/\partial x_j + C_{1\varepsilon}\rho\varepsilon G_k/k - C_2\rho\varepsilon^2/k \quad (2)$$

In these equations, G_k represents the generation of turbulence kinetic energy due to the mean velocity gradients, calculated by:

$$G_k = \mu_t/\rho * \partial u_i(\partial u_i/\partial x_j + \partial u_j/\partial x_i)/\partial x_j \quad (3)$$

The k and ε are coupled to the governing equations via the relation

$$\mu_t = \rho C_\mu k^2/\varepsilon \quad (4)$$

The empirical constant for the turbulence model are assigned the values in accordance with the recommendation of Launder and Spalding[5].

$C_{1\varepsilon}$= 1.44, $C_{2\varepsilon}$ = 1.92, C_μ=0.09, σ_k= 1.0, σ_ε=1.3

The simulation in heat exchanger

The heat exchanger blocks are treated as porous medium in calculating the flow resistance. The porous media parameters could be deduced by the correlation between the velocity and pressure differential, which could be obtained from given empirical correlations of friction factor f, and the definition of friction factor f [6].

The heat exchanger models in ANSYS FLUENT 14.5 are used to simulate the heat dissipation, where the heat exchanger blocks are considered as m*n sub-elements and the Number of Transfer Units (NTU) is calculated in each element. The method proceeds by calculating the heat capacity rates (i.e. mass flow rate multiplied by specific heat) and for the hot and cold fluids respectively, and denoting the smaller one as $C_{\min}$, the larger one as $C_{\max}$.

Then the heat capacity ratio

$$C^* = \frac{C_{\min}}{C_{\max}} \quad (5)$$

The effectiveness E:

$$E = 1 - \exp(\frac{NTU^{0.22}}{C^*}[\exp(-C^* NTU^{0.78}) - 1]) \quad (6)$$

Set the mass-averaged temperature of the heat exchanger boundary as the inlet temperature of sub-element, the heat transfer rate of each sub-element is:

$$q_{micro} = EC_{\min}(T_{in.auxiliary} - T_{in,primary}) \quad (7)$$

The total heat flux of the heat exchanger could be written as:

$$q_{total} = \sum_{i=1}^{i=n}\sum_{j=1}^{j=n} q_{micro,i,j} \quad (8)$$

Fan model and the validation

The Multiple Reference Frame (MRF) model is used to simulating the flow motivated by fan. The multiple reference coordinate systems are built in the fan region, and re-built with the flow circulation. The velocity vectors in multiple reference coordinate systems could be changed from [7]:

$$\vec{v_r} = \vec{v} - (\vec{v_t} + \vec{\omega} \times \vec{r}) \quad (9)$$

Where $\vec{v_r}$ is the reference velocity vector in moving coordinate systems, $\vec{v}$ is the velocity vector in absolute coordinate system, $\vec{v_t}$ is the movement of moving coordinate system, and $\vec{\omega}$ is the angular speed of a rotation.

Thus the mass conservation and momentum conservation equation in this region could be written as:

$$\partial\rho/\partial t + \nabla\cdot\rho\vec{v_r} = 0 \quad (10)$$

$$\partial\rho\vec{v}/\partial t + \nabla\cdot(\rho\vec{v_r}\vec{v}) + \rho[\vec{\omega}\times(\vec{v} - \vec{v_t})] = -\nabla p + \nabla\bar{\bar{\tau}} + \vec{F} \quad (11)$$

The MRF model has been widely used in simulating the full-sized three-dimensional fan[8~13]. To validate the fan model adopted in this paper, we built and calculate the fan at first. The computational domain adopted here is cylindrical, and its diameter equals to the diameter of fan cover. The inlet is 4 times of the diameters upstream to the fan, and the outlet is 6 times of the diameters downstream. Figure 4 displays the sketch of fan model and the surface meshes. Figure 5 show the streamlines in the fan model, where the streamlines are coloured by velocity magnitudes. The swirl flow driven by the fan could be clearly observed here, and the higher speed flow is close to the tip of fan blades.

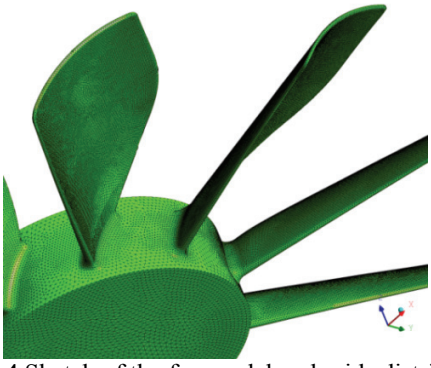

Figure 4 Sketch of the fan model and grids distribution

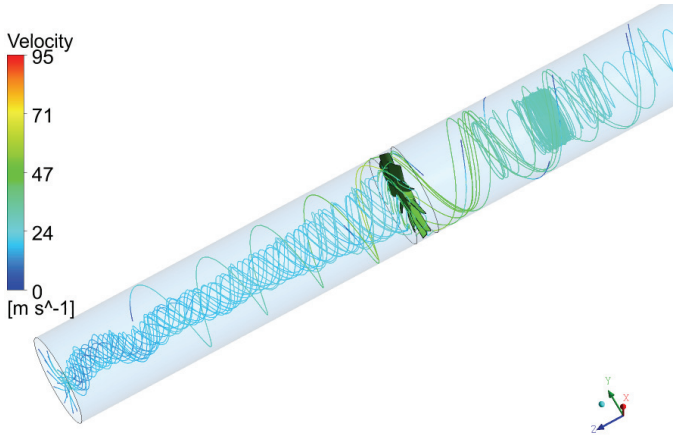

Figure 5 Streamlines in fan model

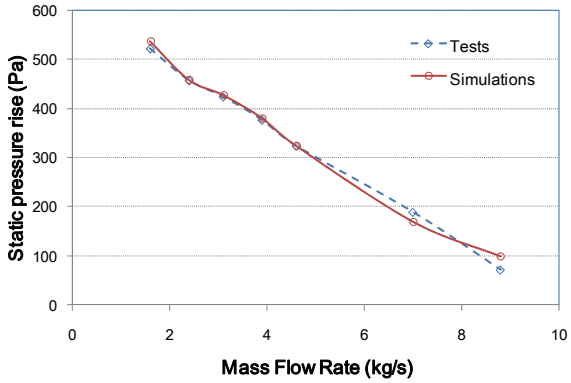

Figure 6 The simulated and test results of fan pressure rise vs. mass flow rate at 1400rpm

The comparison of the simulating results and fan test results is shown in Figure 6. According to this figure, the simulating results match the tests very well with the maximum error is less than 5%. It proves that the calculations on the fan by MRF model are credible.

RESULTS AND DISCUSSION

The flow fields in detached cooling-compartment

Seven cases with the fan speed be adjusted from 1200rpm to 2400rpm are calculated for comparison. The Figure 7 displays the streamlines in detached cooling-compartment at various models and fan speeds. The orange lines represent the flow from inlet1 and the blue lines depict the flow from inlet2. From this figure, the heat exchangers have similar functions as rectifiers in the flow fields of both models. Compared to the flow in parallel model, the mixture in opposite model is comparatively less with the influence of heat exchangers at the inlets, and the swirl only occurred in the region close to the fan.

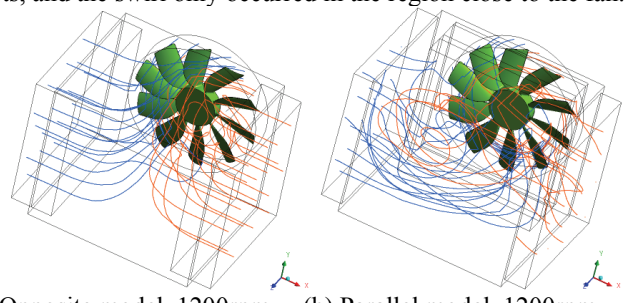

(a) Opposite model, 1200rpm (b) Parallel model, 1200rpm

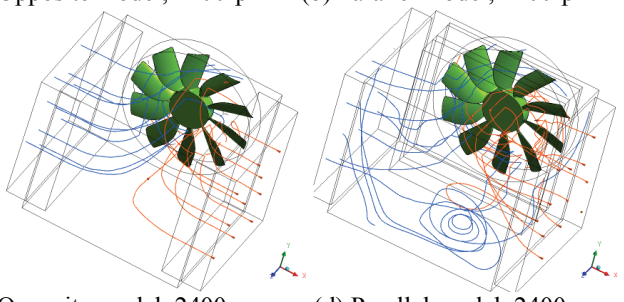

(c) Opposite model, 2400rpm (d) Parallel model, 2400rpm

Figure 7 Streamlines in the detached cooling-compartment at different fan speeds.

When the fan speeds are increased, the flow in opposite model has no obvious change, and the one in parallel model looks very turbulence also. Figure 8 is the top view showing the coloured contours of pressure with surface streamlines in the mid-plane. From the Figure 8(b) and (d), the flows in the bottom of parallel model (lower than the heat exchangers) change direction several times before arriving the fan and outlet. Backflows might be happened in parallel models' inlets. Thus the mass flow rate calculated from outlet in parallel model is far less than the one in opposite model, as plotted in Figure 9.

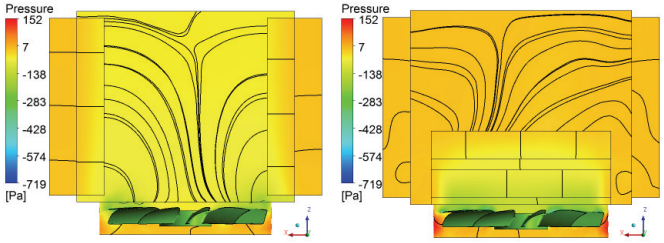

(a) Opposite model, 1200rpm (b) Parallel model, 1200rpm

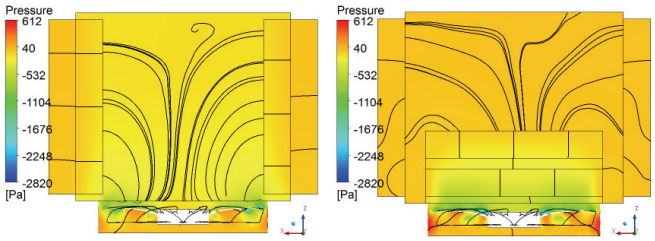

(c) Opposite model, 2400rpm (d) Parallel model, 2400rpm

Figure 8 Pressure distribution and surface streamlines in the mid-profile at different fan speeds. From this angle, the HE1 is in the left side and HE2 is in right side for Opposite model.

In parallel model, as displayed in Figure 8(b) and (d), the low-pressure area is concentrated in the region from heat exchangers to fan blades, the pressure drop through heat exchangers is added with the pressure drop induced by flow disorder, which make its fan pressure rise is lightly higher than the one in opposite model (Figure 10).

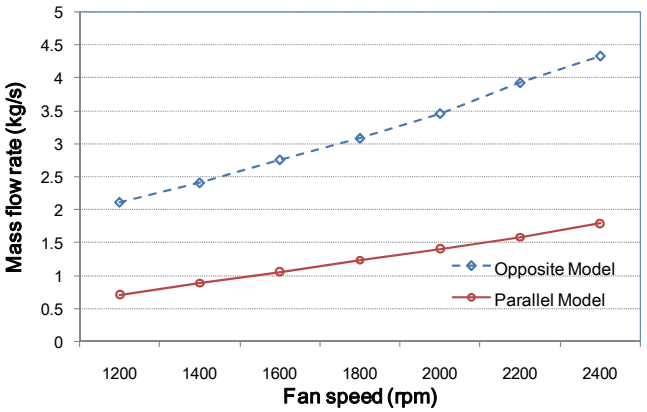

Figure 9 Mass flow rates at various fan speeds

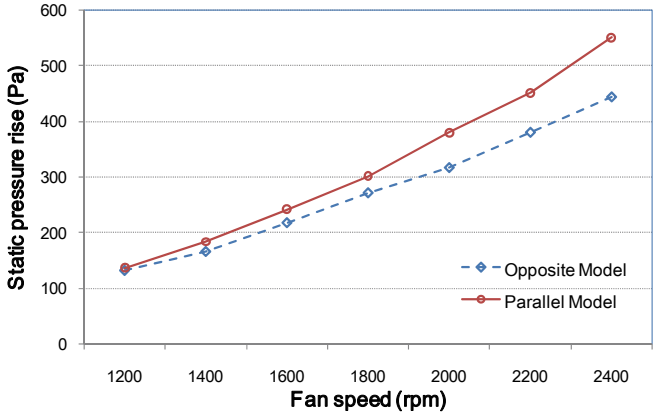

Figure 10 Static pressure rise of the fan at various fan speeds

Analysis of the heat exchange performance

The following figures (Figure 11) illustrate the temperature distributions inside the cooling-compartment. Some surface stream-lines are supplemented to help to analysis the relationship of flow and thermal conditions. We have set the heat exchanger model HE2 as radiator (water-air heat exchange) and the HE1 as intercooler (gas-air heat exchange), it means the intensity of heat transfer in HE2 would be much higher than the one in HE1. From Figure11 (a) and (c), it is noticed that the temperature distributions are coincident with the shape of streamlines in some degree at the opposite models. Which might because the flows among the heat exchangers and fan are barely mixed, the heated air arrive to the fan directly. But in the parallel model, this rule can no longer exist. There are some high temperature areas in the lower part of inlets, what proves that the backflows are existed here.

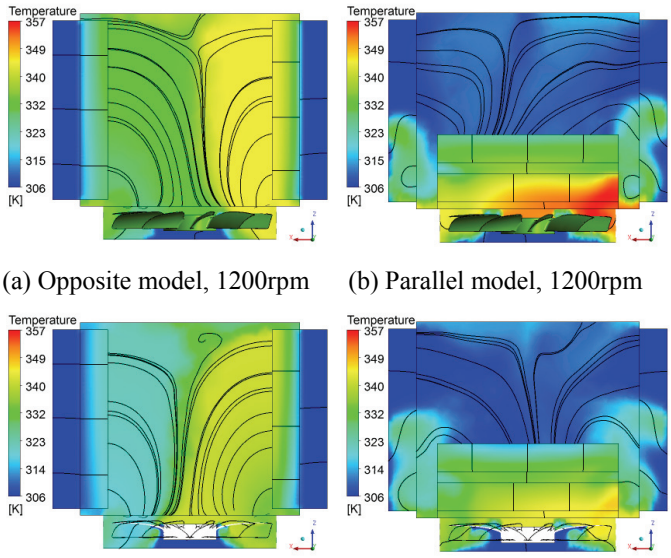

(a) Opposite model, 1200rpm (b) Parallel model, 1200rpm

(c) Opposite model, 2400rpm (d) Parallel model, 2400rpm

Figure 11 Temperature distribution and surface streamlines in the mid-profile at different fan speeds. From this angle, the HE1 is in the left side and HE2 is in the right for Opposite model.

The thermal status inside compartment also could be observed in Figure 11. When the fan speed is increased, the mass flow rate is amplified accordingly, thus the temperature distributed in heat exchangers is obviously decreased.

Figure 12 plots the heat rejections of each heat exchanger in both models at various fan speeds. OM in the legends represents the opposite model, PM represents the parallel model. From this figure, the heat rejections in opposite model are considerably larger than the one in parallel model at all fan speeds. The gap of HE2 between two models is even more apparent. In parallel model, when the fan speed is less than 1400 rpm, the cooling air has relatively small volume and it is easily to be heated in the upstream, thus the heat rejection in HE2 is even smaller than the one in HE1. But when the fan speeds are increased, the growth of heat rejection in HE2 is clearly higher than in HE1. This may indicate that the highest cooling capability is determined not only by the mass flow rate but also by the heat transfer mediums. For the water-gas heat exchangers, like radiator, the thermal heat capacity of water is much larger than the one of air. Then the increasing of air mass flow can improve the cooling performance effectively. But for the gas-to-air heat exchanger, such as intercooler, if the hot-side flow conditions have been fixed, the heat transfer performance can be promoted only in a limited range by amplifying the cooling air volume.

Based on this study, we could deduce that the requirements on the air volume for various heat exchangers to gain enough cooling effects are different. If we can manipulate the air mass flow for each heat exchanger specially, according to their requirements, the efficiency would be improved. And the opposite model in detached cooling-compartment offers us such an opportunity. Calculate the required cooling air volume for each heat exchangers, adjust the mass flow rate by shutters or some other facilities accordingly, then the flow in cooling-compartment could be more close to the idealistic state.

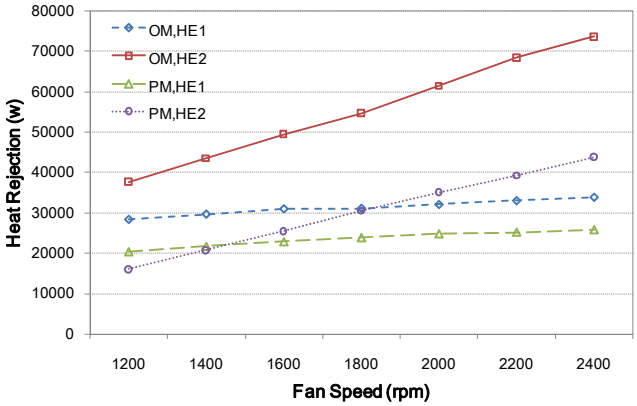

Figure 12 Heat rejections of heat exchangers at various fan speeds

The cooling efficiency was calculated by the ratio of total heat rejection and fan's pressure rise, as plotted in Figure 13. The efficiency in opposite model was found to be far greater than the one in parallel model, almost twice as the latter. Although the design for the parallel model here might not be

most reasonable, but the flow structure determined, the flow in parallel model was more unorganized. For opposite model, the backflow was less, the interference between heat exchangers was prevented, and the mass flow on each heat exchanger could be arranged independently. Considering such advantages, the opposite model in cooling-compartment deserves more attentions and applications in future vehicles.

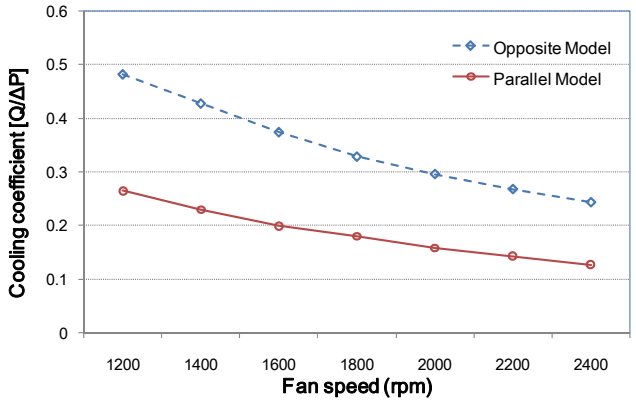

Figure 13 Cooling performance at various fan speeds

CONCLUSION

This paper focused on the flow distributions and heat transfer characteristics in detached vehicular cooling-compartment. Two compartment models both including the heat exchangers and full-sized fan model were established, simulated, and analyzed accordingly. In the opposite model, the heat exchangers are located separately and close to the inlets. In parallel model, two heat exchangers are arranged adjacently and parallel to the fan. The simulation results revealed that:

1. The flow in opposite model is much more organized, and the mass flow rate in it is far larger than the one in parallel model at same fan speed. Yet the fan pressure rise in parallel model is lightly higher than in opposite model.

2. In all fan speeds, the heat transfer efficiency in opposite model is much better than the one in parallel model.

3. On both models, when the fan speeds are increased, the growth of heat rejection in HE2 (which is set according to a radiator) is clearly higher than in HE1 (which is set according to an intercooler). This may indicate that the highest cooling capability is determined not only by the mass flow rate but also by the heat transfer mediums.

Based on the research, for various heat exchangers in the vehicular cooling-system, the requirements on the air volume flow to gain enough cooling effects are totally different. There is a necessary to control the air mass flow independently for each heat exchanger to meet their requirements. The opposite model of detached cooling-compartments has lots of advantages in controlling the flow and improving the cooling efficiency, which deserves more attentions in the future studies.

FUTURE DISCUSSIONS

The present study has revealed that the required cooling-air volumes are definitely different for various heat exchangers to gain the idealistic performance. That means the capability of adjust the flow rate on each heat exchanger individually is useful and valuable for the vehicular cooling system. Thus, there are some works will follow this study aiming to further improve the performance of detached cooling-compartments, such as the comparisons on the different thermal status when the heat conditions are changed, the explores on the idealistic flow distributions, the combination of the natural flow with the fan-driven flow, and the study on fan lay-out strategy etc.

Acknowledgement

This study was supported by an NSFC grant (No.51206141) awarded to the first author.

REFERENCES

[1] Larsson L. , Wiklund T., and Löfdahl L. Cooling Performance investigation of a rear mounted cooling package for heavy vehicles, *SAE Technical Paper* 2011-01-0174, 2011, doi:10.4271/2011-01-0174.

[2] Khaled M., Mangi F., and Hage H. E., Fan air flow analysis and heat transfer enhancement of vehicle underhood cooling system–Towards a new control approach for fuel consumption reduction. *Applied Energy*, vol.91, pp. 1439-1450, 2012

[3] Song H., Guo-dong L., Xiao-li Y. Frame of Construction Machinery Cooling System. Chinese Patent: ZL200920116819.9, 2010.

[4] Song H, Guo-dong L, Xiao-li Y. Intelligent Engineering Mechanical Cooling System[P]. Chinese Patent: ZL200920116820.1, 2010.

[5] Launder B., Spalding D. B., Mathematical Models of Turbulence. *Academic Press*, London, England, 1972.

[6] Huang Y. Q., Huang R., Yu X. L., Lv F. Simulation, experimentation, and collaborative analysis of adjacent heat exchange modules in a vehicular cooling system. *Journal of Zhejiang University, Science B (Applied Physics and Engineering)*, vol.14, pp.417-426, 2013 [doi:10.1631/jzus.A1300038]

[7] ANSYS FLUENT ANSYS. 12.0 User's Guide. ANSYS Inc, 2009

[8] Wang A., Xiao Z., Ghazialam H. Evaluation of the Multiple Reference Frame (MRF) Model in a Truck Fan Simulation. *SAE Technical Paper*, 2005-01-2067, 2005

[9] Kohri I., Kobayashi Y., Matsushima Y. Prediction of the Performance of the Engine Cooling Fan with CFD Simulation. *SAE Technical Paper*, 2010-01-0548, 2010

[10] Gullberg P., Löfdahl L., Adelman S., Nilsson P. An Investigation and Correction Method of Stationary Fan CFD MRF Simulations. *SAE Technical Paper*, 2009-01-3067, 2009

[11] Gullberg P., Löfdahl L., Nilsson P., Adelman S. Continued Study of the Error and Consistency of Fan CFD MRF Models. *SAE Technical Paper*, 2010-01-0553, 2010

[12] Kobayashi Y., Kohr I., Matsushima Y., Study of Influence of MRF Method on the Prediction of the Engine Cooling Fan Performance. *SAE Technical Paper*, 2011-01-0648, 2011

[13] Gullberg P., Sengupta R. Axial Fan Performance Predictions in CFD, Comparison of MRF and Sliding Mesh with Experiments. *SAE Technical Paper*, 2011-01-0652, 2011